ADVANCED SUSTAINABLE SYSTEMS
www.advsustainsys.com

Integrated Environmental and Exergoeconomic Analysis of Biomass-Derived Maleic Anhydride

Jorge Blanco, Maria Linares, Manuel López Granados, Ion Agirre, Iñaki Gandarias, Pedro Luis Arias, Jose Iglesias, Jovita Moreno, and Alicia García**

Life cycle analysis and exergy analysis are applied to compare the production of maleic anhydride from different feedstock, both biomass- and petrochemical-derived raw materials, in order to evaluate the sustainability of alternative biorefinery processes to conventional routes. The considered processes involve two options: gas and aqueous phase furfural oxidation with oxygen (air) and hydrogen peroxide as oxidants, respectively, considered as sustainable technologies because of the use of renewable feedstock. Conventional routes, used as benchmarks, include the current production processes using benzene or butane as raw materials. The results show that the aqueous phase process is far from being viable from an energy and environmental point of view due to the high exergy destruction and the use of H_2O_2 as oxidant (whose production entails important environmental drawbacks). On the contrary, the gas phase oxidation of furfural shows competitive results with petrochemical technologies. Nevertheless, the major environmental drawback of the new furfural-to-maleic anhydride production processes is detected on the environmental profile of the starting raw material. The results suggest that a better environmental footprint for maleic anhydride production in gas phase can be obtained if environmentally friendly furfural production technologies are used at the commercial scale.

1. Introduction

More than 150 years of uninterrupted use of fossil resources, notably accelerated in recent decades, and the consequent emission of greenhouse gases (GHG) has caused, according to the latest report of the IPCC of the United Nations,[1] the already inevitable climate change. This change, which entails a notable increase in the average temperature of the planet, the modification of the rainfall regime, and the increase in the frequency of extreme climatic events, can be all the more pronounced the higher the greenhouse gas emissions continue to be.[1] The reduction of GHG emissions involves addressing a profound change in the use of starting resources, not only for energy uses, but also for the manufacture of different products, moving from an economy based on the use of fossil resources, to another in which renewable resources play a leading role.[2,3] Today, lignocellulosic biomass is one of the few renewable sources of carbon capable of, by availability, replacing crude oil as a raw material for industrial chemical processes.[4] However, transitioning between a crude oil-based economy and bioeconomy requires the development of new biorefinery processes as efficient, profitable, and environmentally sustainable alternatives to crude oil refinery.[5,6]

Maleic anhydride (MAN) is the third most traded aldehyde in the world, only behind phthalic and acetic anhydride, finding numerous applications such as the preparation of unsaturated polyester resins and polymeric materials for construction, coatings, and as starting point for the preparation of a wide variety of chemicals. The most widespread methods for the preparation of maleic anhydride use benzene or butane as raw materials and vanadium phosphorous oxides (VPO*x*) as catalysts. The benzene-based process was the first to be developed,[7] but it has now been replaced, except for small plants, by the butane-based process,[8] due to its higher profitability and better atom economy. Notwithstanding, MAN can be produced from biomass-derived renewable chemicals in biorefinery units, instead of from petrochemical feedstock. For this purpose, several synthetic routes have been developed, using biomass-derived platform molecules. Synthetic strategies starting from levulinic acid[9] or furfural,[10,11] carried out in both liquid and vapor phase reaction conditions have been described. However, these new processes have

J. Blanco, M. Linares, J. Iglesias, J. Moreno, A. García
Chemical & Environmental Engineering Group
Universidad Rey Juan Carlos
C/ Tulipan s/n., Mostoles 28933, Spain
E-mail: jose.iglesias@urjc.es; alicia.garcia@urjc.es
M. López Granados
Institute of Catalysis and Petrochemistry (CSIC)
C/Marie Curie, 2, Campus de Cantoblanco, Madrid 28049, Spain
I. Agirre, I. Gandarias, P. L. Arias
Department of Chemical and Environmental Engineering
Faculty of Engineering Bilbao
University of the Basque Country (UPV/EHU)
Plaza Torres Quevedo 1, Bilbao 48013, Spain

The ORCID identification number(s) for the author(s) of this article can be found under https://doi.org/10.1002/adsu.202200121.

DOI: 10.1002/adsu.202200121

hitherto been studied at a laboratory scale and have not yet made the leap to an industrial scale. In this way, these biorefinery processes, like many others, still have a long way to go to reach the profitability of conventional petrochemical processes and the analysis of the same are associated to large uncertainty.[12] On the other hand, biorefinery processes such as the production of MAN from furfural or levulinic acid are, unlike those making use of benzene and butane, considered as sustainable production technologies,[13] as they are linked to the use of raw materials and intermediates that tend to show low toxicity and high biodegradability. Nevertheless, this is not always the case, and the fact that a product (or a bioproduct) can be produced from a renewable raw material, does not ensure that both the product and the production process are environmentally sustainable.[14] This makes necessary, analysis tools that allow for the qualification of both refinery and biorefinery processes to determine their technical feasibility and sustainability from economical, energy, and environmental points of view. In this context, the use of powerful analysis tools, like life cycle analysis (LCA)[15] or exergy analysis (ExA),[16] or their combination in exergoenvironmental analysis,[17–19] allows a thorough assessment of the sustainability of a process and its fair comparison with analogous processes, producing the same or similar products.

LCA is an internationally standardized and validated methodology conventionally used to evaluate and quantify the environmental impacts of processes. LCA provides a clear picture of the energy and material needs of a process and the environmental releases it causes, that is, its environmental footprint. Standardized methodologies, such as ISO 14044,[20] have made of LCA a reference tool to reach sustainability goals and secure energy supplies in all sorts of processes, including biorefineries.[21] On the other hand, exergy analysis is a powerful tool providing useful information about the efficiency in the use of energy. Exergy analysis allows identifying, locating, and quantifying of thermodynamic inefficiencies or irreversibilities in any type of process involving the use of energy.[22,23] The use of ExA is not so extended as in the case of LCA, but this type of methodologies has attracted great attention to assist in the development of new chemical processes, incorporating energy efficiency constraints to the process design stages.[24,25] Within this context, we present the combined analysis, through ExA and LCA tools, of several chemical processes devoted to the production of maleic anhydride. The purpose of this study is to characterize novel technologies for MAN production, based on the use of furfural as feedstock, from the exergoeconomic and environmental perspectives. Applying standardized ExA and LCA methodologies allows a fair comparison between these new processes and those already existing, based on the use of petrochemical feedstock, allowing the identification of the main weaknesses of the new technologies, regarding their sustainability, to be overcome before their leap to industrial scale.

2. Methodology

2.1. Processes Description

The processes evaluated in this work have been previously described in the techno-economic analysis and comparison of furfural-based routes for maleic anhydride production, using furfural as the starting raw material.[12] These strategies are interesting alternatives to conventional MAN production processes starting from butane or benzene,[26] with the potential to provide a highly demanded commodity through environmentally friendly routes. The analyzed processes consist of both gaseous (MAN(g)) and aqueous phase (MAN(a)) maleic anhydride production processes in which furfural undergoes selective partial oxidation using oxygen (air) and hydrogen peroxide as oxidants, respectively. Briefly, the gas phase process (**Figure 1**A) consists of three different sections, one devoted to thermally conditioning feedstock, the reaction section, and the purification section. Raw materials (air and furfural) are warmed up to the reaction temperature using a series of heat exchangers (E-100–E-102), which take advantage of the high temperature of the reaction products stream. The temperature of each reactant stream, air and furfural, is adjusted in a combustion furnace (H-100 and H-101), burning natural gas as energy source. The mixture of reactants is fed to a jacketed fixed bed reactor (R-100), filled with the oxidation catalyst (V_2O_5 on alumina, 18.6 t), in which the highly exothermic reaction heat is removed, producing medium pressure steam. The stream coming out from the reactor is cooled down by heat exchange with the starting feedstock and fed to an absorption tower (T-100) in which MAN is captured using dibutyl phthalate (DBP) as absorbent. The bottoms of the absorption tower, containing MAN-rich DBP, are then separated in a distillation column (T-101) to recover MAN (head product) and regenerated DBP (bottoms), which are recycled to the absorption tower, with prior heat exchange with the starting air stream (E-100). The aqueous phase process (Figure 1B) consists of a more complex topology, especially in the case of the purification section to obtain MAN. Furfural and an aqueous stream of H_2O_2 (50 wt%) are fed to a fixed bed adiabatic reactor (R-200) filled with the oxidation catalyst (titanium silicate, 63 t). The stream coming out from the reactor is then sent to a distillation train to separate the different reaction products. The distillation train consists of a first stage in which water is removed as head product (T-200), with the help of *o*-xylene, which acts as entrainer. *o*-Xylene forms a low boiling point azeotrope, which separates in D-200 after condensing, being *o*-xylene recycled to the tower while water is removed. The bottoms of T-200 are fed to a second distillation column in which the remaining water and *o*-xylene are separated and sent to decanter D-201. The bottoms of T-201, containing the reaction products, are fed to a third distillation tower (T-202), in which MAN is separated as head product. Finally, the organic phase separated in D-201 is fed to a fourth distillation tower (T-203) to recover *o*-xylene which is recycled to D-200. Operating conditions for the different units of MAN(g) and MAN(a) production processes are listed in Table S1, Supporting Information.

2.2. Exergoeconomics Analysis

2.2.1. Exergy Calculations

The total exergy rates ($\dot{E}x$) of the processes streams have been calculated as the sum of the physical ($\dot{E}x^{ph}$) and chemical ($\dot{E}x^{ch}$) exergy rates, considering the following assumptions:

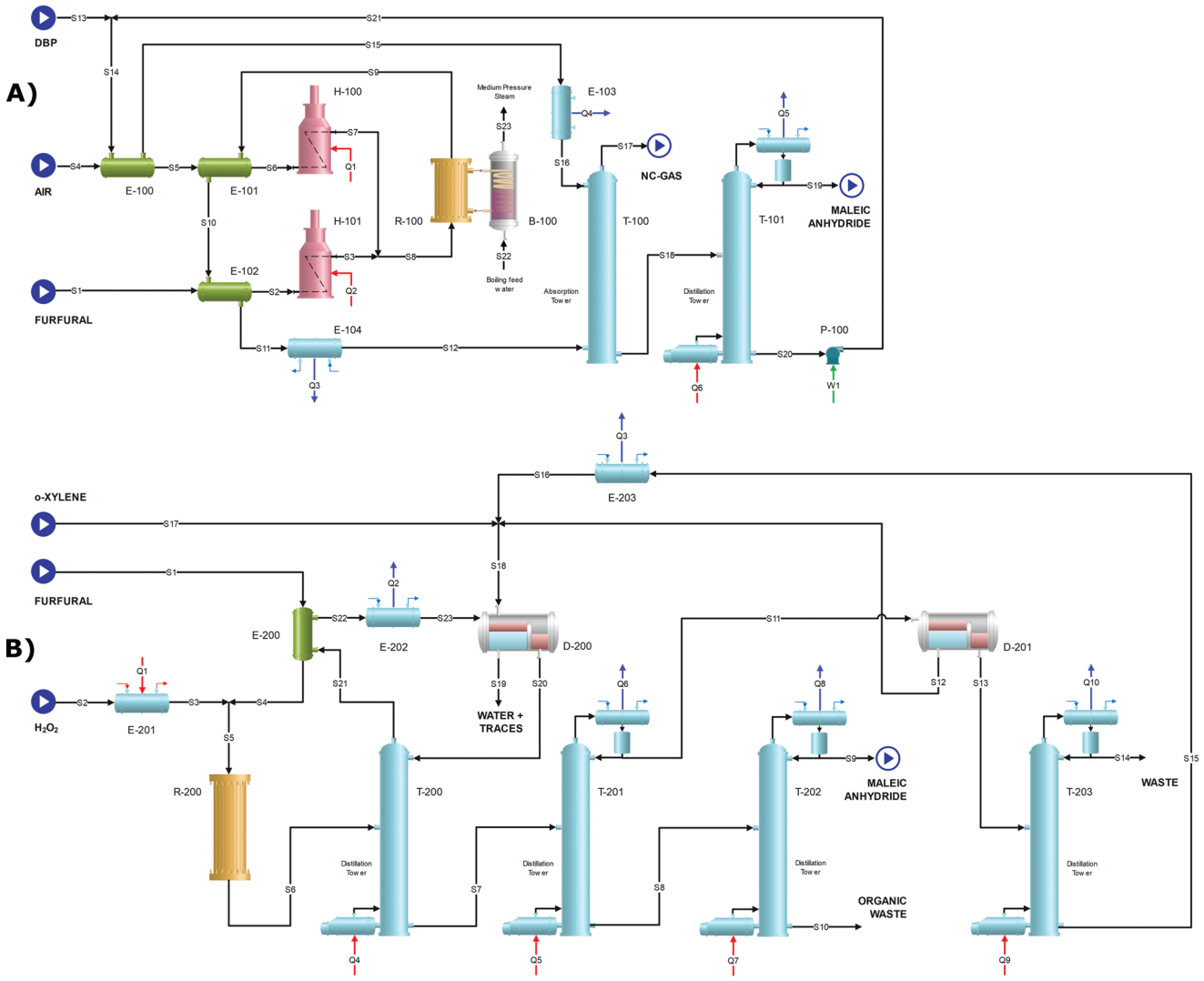

Figure 1. A) Scheme for the designed gas phase maleic anhydride (MAN(g)) production process from furfural. B) Scheme of the designed aqueous phase maleic anhydride (MAN(a)) production process from furfural.

a) All the components of the system (reactors, unit operations, etc.) operate under steady-state conditions.
b) Temperature (T_0) and pressure (P_0) conditions for the dead state were stablished at 298.15 K and 100 kPa, respectively.
c) Standard chemical exergies were calculated using the model proposed by Szargut[27] and applying the revision by Rivero and Garfias.[28]
d) Exergy associated with heat streams was calculated considering the Carnot efficiency: $\dot{E}x^{Q} = \left(1 - \frac{T_0}{T}\right) Q$ (here $T_0 = 298.15$ K, T the temperature of the location where the heat transfer occurs, and Q the transported heat rate).
e) Electrical energy streams are considered 100% exergy.

The main physical and thermodynamic properties and exergy rates of the material streams (Tables S2 and S3, Supporting Information) and the exergy rates associated with heat and electrical streams (Tables S4 and S5, Supporting Information,) were obtained from primary data previously reported for furfural to MAN processes,[12] applying the calculation procedures described above.

Knowing the total exergy rates associated with material and energy streams, the exergy balance of each system component (k) can be written as follows:

$$\dot{E}x_{R,k} = \dot{E}x_{P,k} + \dot{E}x_{W,k} + \dot{E}x_{D,k} \quad (1)$$

where $\dot{E}x_{R,k}$, $\dot{E}x_{P,k}$, $\dot{E}x_{W,k}$, $\dot{E}x_{D,k}$ refer to the total exergy rates of the used resources, associated with the product (or products), lost as wastes and destroyed by irreversibilities, respectively. Accordingly, the exergetic efficiency of component k, where component refers to a process subunit, can be calculated as:

$$\varepsilon_k = \frac{\dot{E}x_{P,k}}{\dot{E}x_{R,k}} \quad (2)$$

2.2.2. Exergy Cost

The exergy cost of a material or energy stream (denoted as Ex*) is defined as the exergy consumed for its production. Thus, for any component k, the exergy cost balance will be written as:

$$Ex^*_{R,k} = Ex^*_{P,k} \tag{3}$$

This makes evident that the exergy cost of the product ($Ex^*_{P,k}$) must be equal to the exergy cost of the consumed resource ($Ex^*_{R,k}$). Equations (1) and (3) make the exergy cost of the resource entirely charged to the product, resulting in a null cost associated to wastes and irreversibilities. Therefore, a high rate of waste generation and exergy destruction conducts to a high $Ex^*_{P,k}/\dot{E}x_{P,k}$ ratio, indicating that for each watt of exergy contained within the product evolving from k equipment, a higher amount of exergy needs to be provided by the fed resource. The $Ex^*_{P,k}/\dot{E}x_{P,k}$ ratio is called unitary exergy cost ($k^*_{P,k}$) and its value provides useful information about the efficiency of the technology linked to the equipment used to produce the considered process stream, so that, more efficient components conduct to lower product unitary exergy costs.

Calculating the exergy cost associated with each process stream requires formulating the exergy cost balance (Equation (3)) for all the components of the process. Table S6, Supporting Information, details the streams defined as resource (R), product (P) and waste (W) for all the components of the evaluated processes for MAN production. However, a process scheme always contains a higher number of streams (n) than components (m), being necessary to find (n–m) additional equations to solve the whole system. In this case, additional equations were accomplished according to the R and P principles described by Lazzareto and Tsatsaronis.[29]

2.2.3. Exergoeconomics Concepts

The combination of economic principles with exergy calculations leads to the exergoeconomic approach. $\dot{C}_{R,k}$ is defined as the cost rate associated with the resource (or resources) used in a process component k, while the cost rate corresponding to the product of this component is written as:

$$\dot{C}_{P,k} = \dot{C}_{R,k} + \dot{Z}_k \tag{4}$$

where $\dot{Z}_k$ is the cost rate associated with the equipment k, considering the capital investment, the operation and maintenance (O&M) cost, and the operation time obtained from primary data previously reported for furfural to MAN processes.[12] Equation (4) also represents the cost balance of the equipment or component k that could be reformulated as follows:

$$c_{P,k}\dot{E}x_{P,k} = c_{R,k}\dot{E}x_{R,k} + \dot{Z}_k \tag{5}$$

where $c_{P,k}$ and $c_{R,k}$ are the unitary exergoeconomic cost of the products and resources, respectively, in component k. This parameter refers to the monetary price of the exergy contained within each stream, that is, $ per Joule of exergy.

Similar to the calculation of the exergy cost associated with each process stream, calculation of the streams cost rates involves formulating an equations system based on the cost balances of all the process components, as well as the additional relations, following the R and P exergoeconomic principles, to cover the degrees of freedom.

Finally, the exergoeconomic factor of each equipment or component k of the process can be defined as follows:

$$f_k = \frac{\dot{Z}_k}{c_{R,k}(\dot{E}x_{W,k} + \dot{E}x_{D,k}) + \dot{Z}_k} \tag{6}$$

where the term $c_{R,k}(\dot{E}x_{W,k} + \dot{E}x_{D,k})$ indicates the cost rate derived from exergy lost and destruction in the considered component (cost of the unproductive exergy) and $\dot{Z}_k$ is the cost of the component, calculated as previously mentioned. Therefore, the f_k factor shows how relevant the cost of the thermodynamic inefficiencies associated to component k is, considering the capital cost needed for its acquisition and operation. A high exergoeconomic factor implies that cheaper, and usually less efficient equipment might be used instead, assuming an increase of exergy destruction but reducing the capital expenditure for the considered component. On the contrary, a low exergoeconomic factor implies that a more efficient technology is required to decrease the unproductive exergy term, but obviously, this usually occurs at the expense of increasing the capital expenditures.

2.3. LCA Framework

Life cycle assessment was conducted for the previously described maleic anhydride processes, following the guidelines provided by the ISO 14044 standard[20] and the ILCD Handbook.[20] Specific methodological aspects are detailed hereunder, based on the ISO 14044 sections.

2.3.1. Goal and Scope

The main goal of the study was to build an environmental profile for both gas and aqueous phase maleic anhydride (MAN) production processes from furfural and their subsequent comparison, both between them and against conventional routes for MAN production from petrochemical feedstock.

At first, a gate-to-gate approach was conducted accounting for the impacts derived from the maleic anhydride plant operation, in accordance with ExA (Section 2.2). Afterward, the scope of the LCA was expanded to cover a cradle-to-gate analysis, including biomass cultivation and harvesting for the production of furfural. This allowed considering the starting feedstock to compare the furfural routes to MAN with conventional processes starting from benzene and n-butane. The corresponding input–output flowchart is shown in **Figure 2**.

The functional unit for LCA was defined as the delivery at the factory gate of 1 tonne > 99.5 wt% pure MAN, and hence, the considered reference flow was 1 tonne of MAN. LCA was performed following an attributional perspective. Although conventional and novel processes take credit for the production of medium-pressure steam (thus avoiding its production from natural gas), no other marginal effects were considered.

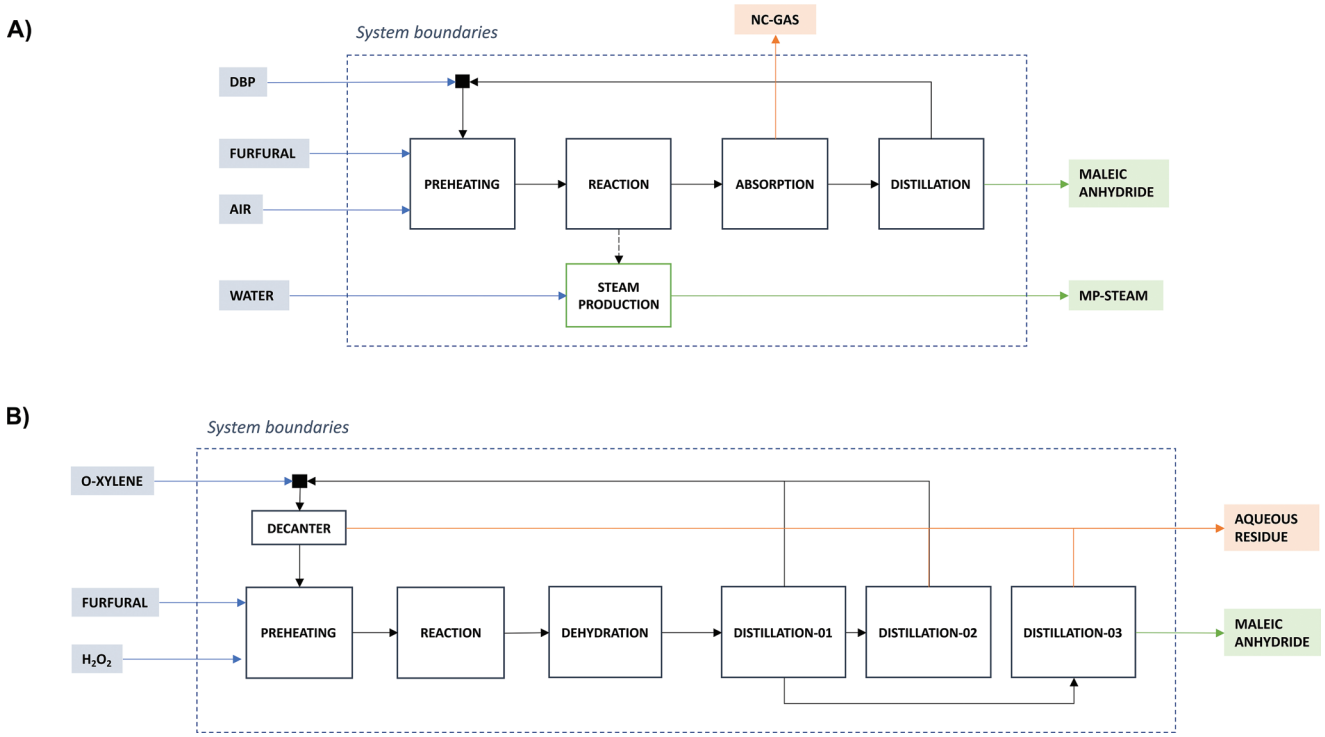

Figure 2. Block diagram for the A) gas and B) aqueous phase maleic anhydride production from furfural.

2.3.2. Life Cycle Inventory (LCI)

A system inventory was built using data retrieved from different sources, regarding the elementary flows shown in Tables S7 and S8, Supporting information. Primary data from Agirre et al.[12] were used for the foreground unit operations in the alternative MAN production routes, whereas GaBi Professional Database (2021 version) was used for the background system. Furfural inventory was further built upon data from Schöppe et al.,[30] based on the Huaxia process (modified by Westpro), which may be regarded as the current dominant process for furfural production.[31,32] In a nutshell, this process consists of the acid depolymerization of the lignocellulosic raw materials (e.g., corncobs) at moderate temperatures (153 °C). Under these conditions, xyloses from the hemicellulosic fraction are dehydrated, and furfural is stripped off the reactor using high-pressure steam as a carrier. Finally, furfural is purified by a double azeotropic distillation.[33,34] Data from the Ecoinvent database (v2.3) were used for the cultivation and harvesting processes for maize production, as well as for transoceanic transportation from China to Europe. Finally, conventional maleic anhydride processes are included in the analysis for comparison purposes. Data for both benzene (MAN(bn)) and n-butane (MAN(bt)) routes had been retrieved from the Ecoinvent database. Additionally, data quality was quantitatively assessed following the Environmental Footprint recommendations provided by the European Commission.[35] An overall "good quality" score was met for both gas and aqueous phase processes. Detailed methodological procedure and disaggregated scores are provided in the Supporting Information.

The carbon balance in the system was systematically reviewed to ensure the validity of the inventory. Carbon input–output inventory for all units in the different furfural-to-MAN processes has been included, together with the Sankey diagram, within the Supporting Information. The assumptions, limitations, and an assertion of the robustness of the LCI are further provided. This assertion includes information on geographical, temporal, and technological data representativeness, as well as the completeness of the inventory.

2.3.3. Life Cycle Impact Assessment (LCIA)

LCIA was performed using the Environmental Footprint (v3.0) methodology implemented in the v10.6 GaBi software. For the sake of clarity, the discussion on the main text is based on the following indicators: acidification (AC, mol H^+ eq), global warming potential (GWP100, Kg CO_2 eq), freshwater ecotoxicity (FWET, CTUe), human cancer effects (HTc, CTUh), human non-cancer effects (HTnc, CTUh), land use (LU, dimensionless), fossil depletion (FD, MJ), and water use (WU, Kg equiv. deprived). Scores obtained for all the EF methodology indicators can be found in the Supporting Information. The biogenic CO_2 is reported separately for the MAN(g), MAN(a), and furfural scenarios, as recommended by the European Commission's Lead Market Initiative[35] for cradle-to-gate studies. The consequences of indirect land use change (iLUC) and biodiversity effects have not been considered in this study.

Valuable outputs, other than maleic anhydride, generated in the main processes (MAN(g) and MAN(a), Tables S7 and S8, Supporting Information), have not been

considered to be recovered and purified, and thus no allocation is required. However, to support a fair comparison between the furfural-based and the conventional processes for MAN production, a system expansion (SE) has been applied, accounting for the credits deduced by the co-production of medium-pressure steam (MP-Steam) generation. SE was implemented for MAN(g), MAN(bn), and MAN(bt) cases, considering the prevention of 3246–6500–7000 kg t^{-1} MAN of steam from natural gas (EU-28 technology mix, 90% efficiency), respectively. In the case of maize, the selected feedstock from Ecoinvent (Grain maize IP, at farm) for furfural production included mass allocation. According to Kromer and Martinov,[36] an average of 10.6 wt% of the weight of maize plants (*Zea mays* L.) correspond to the bare cob, and thus a factor of 0.106 was applied to allocate the impacts of the cultivation and harvesting phases. Detailed results are presented within the Supporting Information.

3. Results and Discussion

3.1. Exergoeconomic Assessment

The exergoeconomic analysis of maleic anhydride production from furfural oxidation in gas (MAN(g)) and liquid phase (MAN(a)) have been carried out to determine the economic performance relative to the results of exergy analysis. This study provides a correlation of the product cost and the exergy invested and destroyed in the designed processes, so that the obtained data can be employed to identify and improve inefficiency in units and process configurations, in terms of exergy cost and efficiency.

3.1.1. Gas-Phase Process

The exergy costs (Ex*), unitary exergy costs (k*), cost rates ($\dot{C}$), and unitary exergoeconomic costs (c) calculated for all the streams involved in the MAN(g) process are listed in **Table 1**. As mentioned, all these parameters provide an idea about the thermodynamic efficiency of a process (Ex*, k*), and the consequences of that performance on the economics of the same ($\dot{C}$,c). Significant differences in terms of exergy costs and unitary exergy costs can be observed between the streams. Larger values for these parameters suggest the existence of inefficiencies in the use of the energy, and thus, from the comparative analysis of the values listed in Table 1, up to three hotspots can be detected: the recovery of DBP, feed air preheating, and the partial oxidation of furfural to MAN accomplished in reactor R-100. The large exergy costs associated with material streams involved in DBP recovery (S14, S15, S16, S18, S20, and S21), located at the end of process (Figure 1A), are due to the addition of inefficiencies during the overall process, which are accumulated and discharged over the process streams at the end battery limits. In this way, maximizing the recovery of DBP is probably the only practical way to avoid large exergy losses associated with this area. Regarding the air preheating section, comprising heat exchangers E-100 and E-101 and furnace H-100, unitary exergy costs of the material streams in this section indicate that this step is showing the highest exergy consumption among all the sections in the process flowchart. The combination of a large air mass flow rate, required to accomplish the partial oxidation of the starting furfural, together with a high temperature increase, seem to be the most plausible reasons for the large unitary exergy costs. However, using the recycled DBP, a highly expensive heat source from an exergy point of view, to condition air temperature, could also be an important contribution of the risk of inefficiency in this area. Together with the preheating of air, the unitary exergy costs of the streams related to oxidation reactor points to the third hotspot at the chemical reactor. This could be a consequence of irreversibilities associated with the considered chemical reactions for furfural to MAN oxidation, which lack atom efficiency (at least 1 carbon atom out from 5 is lost as CO_2).

The cost rate of the different streams, as an economic factor, can be considered as a direct measurement of the economic efficiency of a process. However, associating the cost rate to each exergy transfer provides the unitary exergoeconomic cost, which is the combination of the monetary cost of the exergy needed to produce a certain stream, together with the costs associated with the productive process (capital investments, maintenance, etc.). This parameter allows for assigning monetary costs to the interactions that a system or equipment experiences with its surroundings and to the sources of thermodynamic inefficiencies within it. In this way, the previously detected thermodynamic inefficient hotspots in MAN(g) process can be also evaluated from an economic point of view. Thus, for instance, from the mass flow of recycled DBP mainstream (S21; 102168 kg h^{-1}) and its economic cost (3761 \$ t^{-1}), one of the largest in MAN(g) process, more than twice that corresponding to the cost of fresh DBP (1785 \$ t^{-1}), it is evident that recycling DBP is a highly expensive operation. In this way, any improvement in the proposed DBP recovery scheme should be considered, as it has a direct impact on the profitability of the overall MAN(g) process.

Unitary exergoeconomic costs of material streams (Table 1) not only point to the aforementioned high cost of recycled DBT but also to those streams involved in air preheating and in the oxidation of furfural to MAN. The high unitary exergoeconomic costs of air preheating are a consequence of the large physical exergy involved in this step: chemical exergy remains constant and the largest value is calculated to air coming out from heat exchanger E-100. In this way, the use of the expensive DBT recycled stream seems also to play an important role in the high c values calculated for conditioned air. A plausible way to alleviate this situation could be optimizing the heat exchange sequence accomplished in heat exchangers E-100 and E-101 and furnace H-100. Finally, the reactor outlet, as well as the subsequent cooled streams, also display high unitary exergoeconomic costs. In this case, the irreversibilities and inefficiencies of the chemical transformation are the main causes for the high exergy destruction. Nevertheless, the influence of the total cost of the reactor should not be discarded in providing a high exergoeconomic cost, as the capital expenditure associate to this component is rather high.

Table S6, Supporting Information, contains the productive structure of MAN(g) process, indicating which stream or combination of streams, constitute products (P), consumed resources, or fuel, (R) and wastes (W) for all the components

Table 1. Exergy cost (Ex*), unitary exergy cost (k^*), cost rate ($\dot{C}$), and unitary exergoeconomic cost (c) of all the streams involved in the gas phase maleic anhydride production process from furfural.

Stream	Ex* [kW]	k^*	$\dot{C}$ [\$ h^{-1}]	c [\$ GJ^{-1}]
S1	33677	1.00	4804	40
S2	34580	1.02	4968	41
S3	34648	1.02	4984	41
S4	179	1.00	0	0
S5	6135	2.81	1207	154
S6	8474	2.61	1641	140
S7	8673	2.51	1670	134
S8	43321	1.17	6654	50
S9	39694	2.13	6587	98
S10	37358	2.13	6199	98
S11	3,6454	2.13	6049	98
S12	36454	2.27	6078	105
S13	24	1.00	50.0	57
S14	2021160	2.25	384219	119
S15	2015205	2.25	383087	119
S16	2015205	2.25	383106	119
S17	0	0	0	0
S18	2051659	2.25	389358	119
S19	33530	2.25	6374	119
S20	2021132	2.25	384203	119
S21	2021135	2.25	384214	119
S22	80	1.00	0	1
S23	3707	1.00	287	22
Q1	202	1.00	13	18
Q2	68	1.00	4.3	18
Q3	0	0	0	0
Q4	0	0	0	0
Q5	0	0	0	0
Q6	3003	1.00	496	46
W1	3.4	1.00	0.3	25

included within the process. From this productive structure, the exergy destruction rate in all the components can be calculated, being the results shown in **Figure 3**A1. The highest exergy destruction rate in MAN(g) process takes place within the chemical reactor, in which 86.5% of the overall invested exergy is destructed. This result evidences the high thermodynamic imperfection of the reaction and the enormous potential for thermodynamic improvement if the chemical transformation is conducted in a higher efficient way. Irreversibilities in the chemical reactor can be ascribed to different reasons, including the deficits of the reaction scheme in carbon atom economy, to the irreversible character of the chemical transformations, and to the high operation temperature required to drive the selective oxidation of furfural to MAN.[37,38] In this way, investing effort in enhancing the performance of the catalytic transformation seems to be an adequate option to improve the efficiency of the core step, the chemical reactor, of MAN(g) process. The rest of the sources for exergy destruction detected in MAN(g) are distributed between the heat exchanger preheating feed air (E-100), the boiler dissipating the reaction heat by steam generation (B-100), and the distillation tower to recover MAN and to regenerate DBT (T-101). However, all these components lead to less than 10% of the total exergy destruction calculated for the overall process. In this way, although trying to improve all these operations is always desirable, the most critical point is still the chemical reactor.

Figure 3A2 depicts a comparison of the unitary exergoeconomic costs of the resources and products streams associated with each component in MAN(g) process. Interestingly, the highest product unitary exergoeconomic cost was obtained in pump P-100 (947 \$ per GJ), despite its negligible exergy destruction. This probably arises from the energy source (electrical power, 100% exergy, 3.4 kW), whose economic cost is directly charged to the pumped product stream. The lowest unitary exergoeconomic costs, on the contrary, are those obtained in the boiler, because the energy needed in this equipment is

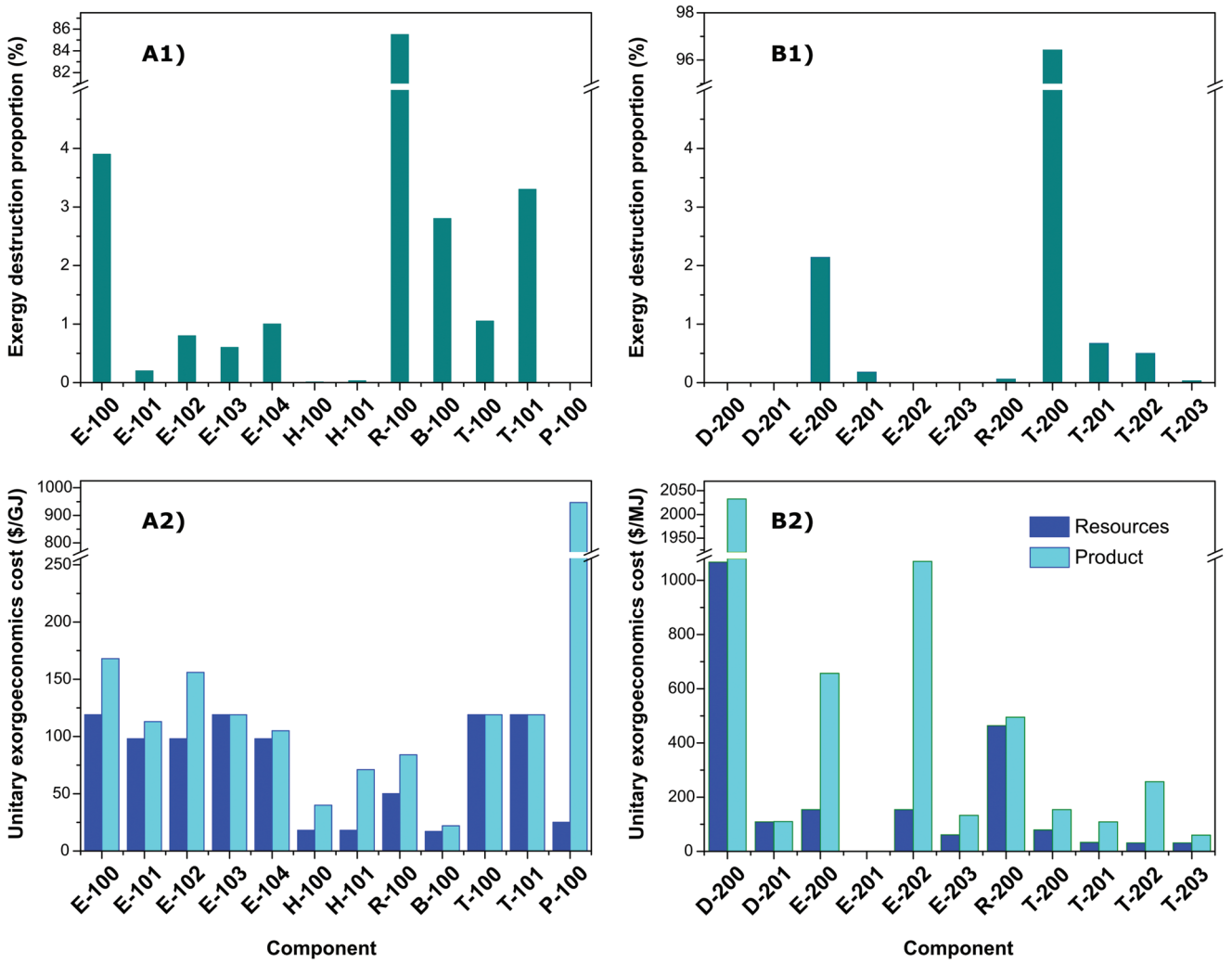

Figure 3. A1) Exergy destruction proportion and A2) unitary exergoeconomic cost of fuel and products of the different equipment involved in MAN(g) process. B1) Exergy destruction proportion and B2) unitary exergoeconomic cost of fuel and products of the different equipment involved in the MAN(g) process.

directly obtained from the exothermic reactions taking place in the chemical reactor. In this way, there is no need of an additional energy supply to produce the medium pressure steam within boiler B-100. The different heat exchangers of the process (E-100, E-101, and E-102) show similar resource unitary exergoeconomic cost, but the unitary exergoeconomic costs attributed to product stream in E-101 are significantly lower, probably because of the lower temperature increase in this unit as compared to other heat exchangers. The unitary exergoeconomic costs of resources in furnaces, which make use of natural gas as energy source (H-100 and H-101), are much lower than those obtained in heat exchangers, because of the lower temperature increase produced in these heaters involving quite a low fuel consumption. Finally, it is noteworthy that, despite the high degree of exergy destruction observed in the chemical reactor, a moderate unitary exergoeconomic cost is obtained, probably because the cost rate associated with reactants in stream S8 is not high.

Table 2 lists the exergoeconomic factors of the different components of the MAN(g) process, meaning the contribution of the cost rate of each equipment with the costs associated with its capital and exergy destruction. Typically, the impact of equipment cost is considered dominant when the exergoeconomic factor is higher than 70%, whereas the irreversibility-related cost is the dominant contribution when the value of exergoeconomic factor is lower than 30%.[39] For the considered process, the calculated exergoeconomic factors ranged between 6.7% and 99.8%. Pump P-100 and the furnaces burning natural gas (H-100 and H-101) displayed the highest exergoeconomic factors with values above 95%, suggesting that capital expenditures associated with the acquisition of these units might be reduced to balance capital and irreversibilities' costs. The same conclusion is obtained in relation to the exergoeconomic factor of heat exchanger E-101 (f_k value of 82.4%). All these components show high exergetic efficiencies (Table 2), due to the low thermodynamic non-idealities associated with the transformations

Table 2. Results of exergy and exergoeconomic analysis of the gas phase maleic anhydride production process from furfural.

Component	$\dot{E}x_W + \dot{E}x_D$ [kW]	c_R [$/GJ]	$\dot{Z}_k$ [$ h^{-1}]	f_k [%]	ε_k [%]
E-100	643	119	75	21.4	75.8
E-101	28	98	46	82.4	97.4
E-102	133	98	14	22.9	68.6
E-103	220	119	20	17.2	99.97
E-104	1053	98	29	7.1	93.9
H-100	2	18	16	99.2	99.0
H-101	5	18	12	97.6	93.4
R-100	14359	50	186	6.7	61.3
B-100	458	17	33	53.8	88.8
T-100	686	119	174	37.3	99.9
T-101	679	119	723	71.3	99.9
P-100	0.19	25	11	99.8	94.3

occurring within the same, so that there is a margin for a decrease in investment costs

3.1.2. Aqueous-Phase Process

Results of the exergoeconomic analysis applied to the liquid-phase process for MAN production (MAN(a)) are listed in **Tables 3** and **4**. As compared to the results previously commented for the MAN(g) process, higher unitary exergy cost values (k^*) are observed. This is caused by two factors: the exergy level of the process and the existence of irreversibilities. Exergy attributed to liquid-phase streams is lower than those in MAN(g) process because of their lower energy level (see Supporting Information and the thermodynamic properties of streams in Tables S3 and S5, Supporting Information). On the other hand, poorly efficient transformations take place in several components of MAN(a) process. One of the most critical steps in this sense, already highlighted by Aguirre et al.,[12] is the azeotropic distillation (T-200) required for maleic acid dehydration. This step involves a huge consumption of energy (see Q4 in Table S5, Supporting Information) due to the high temperature of the boiler at this column (161 °C), being the main cause of exergy destruction.[40] Accordingly, results shown in Figure 3B1 highlight the high contribution of the distillation column T-200 to exergy destruction, which accounts for more than 95% of the total exergy destruction in the MAN(a) process. Taking into account not only exergy destruction but also exergy loses, it must be considered that an important part of the energy fed to column T-200 is removed in heat exchanger E-202, devoted to condensate the distillate stream (S22). Despite a small fraction of the energy contained in the vapor phase distillate (S21) being recovered in E-200 for furfural preheating (from 25 °C to 50 °C), energy transferred within this equipment barely takes advantage of the latent heat associated with condensation. Therefore, almost all the energy invested in the distillation column T-200 is removed in E-202, thus generating a waste heat flow (Q2) with no subsequent use of its exergy. This is the reason why the streams coming from both, the T-200 column and the heat exchanger E-202 (S21, S22, and S23), have all of them very high unitary exergy costs. Besides, all these exergy destruction and losses are finally charged on the organic stream generated in decanter D-200 (S20), as the aqueous stream (S19) was also considered as a residue (its exergy cost is zero). Stream S20 is refluxed back to the head of the column T-200, closing the cycle of streams with such high unitary exergy costs.

Considering the economic aspects, the cost rates and the exergeconomic costs associated with the streams of the aqueous-phase production process (Table 3) are much higher than those obtained for the gas-phase system (Table 1). This is not only due to exergy destruction and losses, as previously commented, but also due to the higher cost of the raw materials required for this synthesis pathway (especially H_2O_2, stream S2). According to the productive structure defined in Table S6, Supporting Information, exergoeconomic analysis provides a cost rate for the stream of maleic anhydride (S9) of 32,30 $ h^{-1}, which involves 9,51 $ t^{-1} MAN, more than five times higher than that obtained for the gas-phase process. It is also remarkable how removing Q2 for the condensation of the distillate (in exchanger E-202) considerably increases the exergoeconomic cost (c) of stream S23 as compared to S22 (product and resource streams in E-202, respectively). This is because S23 stream contains much less energy (liquid state) and it adds the total cost rate of both, resource ($\dot{C}_R$) and equipment E-202 ($\dot{Z}$) (as Q2 is considered as a residue, as it is not further used within the process), resulting in a much higher cost of each exergy unit in this stream. Differences between exergoeconomic costs (c) of resources (R) and products (P) of each unit of the process are displayed in Figure 3B2. One of the largest differences between c_P and c_R is obtained for the heat exchanger E-202, with an increase of almost seven times of c_P as compared to the starting c_R indicating again that removing Q2 without any further use of this heat flow is one of the most critical points that affects the exergoeconomic performance of the process. In general, the lack of use of extracted heat streams in the cooler (E-202) and column condensers, which are considered as residues (Q2, Q3, Q6, Q8, and Q10), leads to important overcosts, finally collected by the products of these units, increasing their exergoeconomic costs. Besides the high price of the raw

Table 3. Exergy cost (Ex*), unitary exergoeconomic cost (c), and cost rate ($\dot{C}$) of all the streams involved in the aqueous phase maleic anhydride production process from furfural.

Stream	Ex* [kW]	k*	$\dot{C}$ [\$ h^{-1}]	c [\$ MJ^{-1}]
S1	8.1	1.0	4259	146
S2	3.2	1.0	19331	1668
S3	74	1.6	19385	116
S4	217041	1995	242484	619
S5	217115	1385	261869	464
S6	217115	1476	262162	495
S7	31753	505	34848	154
S8	29316	358	32124	109
S9	29526	844	32304	257
S10	0	0	0	0
S11	2672	358	2928	109
S12	24	358	27	110
S13	2648	358	2940	110
S14	0	0	0	0
S15	2667	192	3061	61
S16	2667	415	3072	133
S17	0	1.0	155	108
S18	2691	429	3254	144
S19	0	0	0	0
S20	7552820	6668	8289935	2033
S21	7767162	505	8524176	154
S22	7550128	505	8285990	154
S23	7550128	3509	8286608	1070
Q1	71	1.0	35	0.14
Q2	0	0	0	0
Q3	0	0	0	0
Q4	28980	1.0	4466	0.04
Q5	234	1.0	45	0.05
Q6	0	0	0	0
Q7	210	1.0	15	0.02
Q8	0	0	0	0
Q9	19	1.0	3	0.05
Q10	0	0	0	0

materials, these non-recovered energy streams undoubtedly contribute to an exergoeconomic performance very far from the optimum. This fact can be verified checking exergoeconomic factor values (f_k) obtained for the different units (displayed in Table 4). In this regard, only decanter D-201 and heat exchanger E-201 show factor values higher than 50%. In the first case, this is because the terms related to exergy loss and irreversibilities ($\dot{E}x_W + \dot{E}x_D$) are null, whereas in the second case, the cost associated with inefficiencies (still bearable) and capital costs are compensated by the location of the equipment at the beginning of the process flowchart (before T-200 column). For the rest of the units, f_k values are all of them lower than 10%, indicating that the cost related to exergy losses and destruction is

Table 4. Results of exergy analysis of the aqueous phase maleic anhydride production process from furfural.

Component	$\dot{E}x_W + \dot{E}x_D$ [kW]	c_R [\$ MJ^{-1}]	$\dot{Z}_k$ [\$ h^{-1}]	f_k [%]	ε_k [%]
D-200	1025	1067	72.2	<0.1	53
D-201	0	109	39.1	100	100
E-200	329	154	29.3	<0.1	23
E-201	27	0.1	19.4	59	61
E-202	12793	154	618	<0.1	14
E-203	7	61	11.7	0.7	46
R-200	10	464	293	1.8	94
T-200	14823	79	2461	<0.1	51
T-201	208	33	159	0.6	30
T-202	257	31	165	0.6	12
T-203	12	31	117	8	53

the dominant parameter in the exergoeconomy of the unit.[41] As mentioned above, operations involving large irreversibilities (e.g., the distillation performed in T-200), huge residual flows (condensation in E-202 or decantation in D-200), and/or expensive reactants, are all of them critical points contributing to the exergoeconomic inefficiency of the liquid-phase alternative for MAN production. Using heat integration methodologies or converting waste into possible co-products (including circular economy principles to the process design) could considerably decrease the exergoeconomic costs of the streams, raising the f_k value closer to an optimum performance. In addition, and bearing in mind the high costs ascribed to H_2O_2, exploring synthesis options using cheaper oxidant reactants would also allow for obtaining more compensated processes according to the exergoeconomic analysis. However, all these options involve considering a completely different chemical process for MAN production from furfural, and thus, from ExA results, it is evident that MAN from furfural using hydrogen peroxide as oxidant and liquid-phase conditions, involve extraordinary drawbacks.

3.2. Life Cycle Assessment

In the following section, LCA results are discussed, first from a gate-to-gate perspective, for an easier parallel integration of the exergoeconomic and life cycle analysis, and afterward, using a cradle-to-gate scope, to evaluate the main points to improve the MAN production process from an environmental point of view. Finally, the proposed processes are compared against benchmark technologies to provide a broader context to the results and to evaluate the readiness of these options to make a leap to industrial scale. Unless otherwise stated, results are presented per tonne of MAN (reference flow).

3.2.1. Gate-to-Gate Boundaries

The environmental performance of the furfural to MAN gas and aqueous phase production processes has been tackled

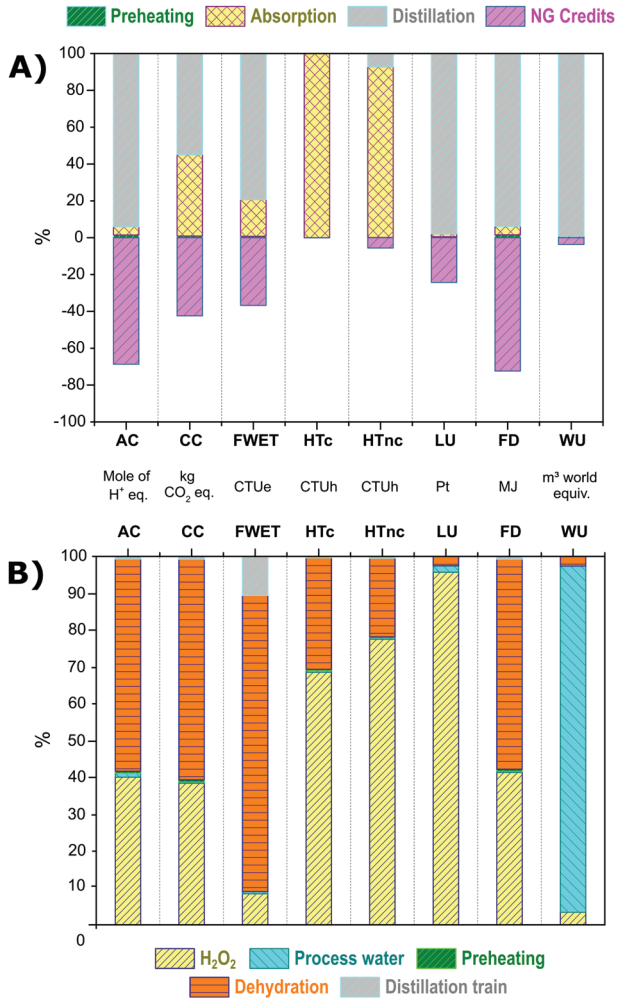

Figure 4. Relative contribution of A) MAN(g) and B) MAN(a) processes to the studied impact categories, considering a gate-to-gate scope. Negative values correspond to MP-Steam credits.

in first term. Starting from the gas phase process, **Figure 4**A depicts the contribution of the unit operations and components in MAN(g) process to the different impact categories in the LCA. A significant contribution of the product separation stages, comprising the adsorption and the distillation train, to most of the studied impact categories, is detected. Within this context, the absorption stage plays an important role in climate change and human toxicity impacts due to the extensive use of DBP. Climate change impacts are mainly due to CO_2 emissions, reaching 448 kg t^{-1} in the case of absorption and 551 kg t^{-1} in the distillation. In the first case, this means the emission of 149 kg t^{-1} of CO_2 per absorption column (three towers operating in parallel[12]), similar to the 137 75 kg t^{-1} of CO_2 emitted per tower in the distillation (four towers in parallel[12]). Considering other greenhouse gases (GHGs) included in the baseline model of the IPCC,[34] the production of MAN through the gas phase process involves a global warming potential score of 1.1 kg CO_2-equiv. kg^{-1} MAN and 0.631 kg CO_2-equiv. kg^{-1} MAN if MP-Steam production credits are deducted (**Table 5**). This value corresponds to the sum of the emissions corresponding to fossil and biogenic carbon, plus the land use (LU) and land use change (LUC) effects, albeit > 99% is associated with the fossil sources.

Human toxicity effects are tightly bound to furan emissions to the atmosphere during the absorption step. As shown in Table S6, Supporting Information, almost 10 kg of furan is released during this phase. Furan is previously formed in the reactor through a side reaction, in which furfural is partially decarboxylated, in accordance to what was previously described by Agirre et al.[12] Alleviation strategies to reduce the importance of absorption step in human toxicity require condensation and treatment of stream S17 (Figure 1A). That would significantly mitigate the toxicity potential and allow a further recovery of the MAN and DBP before being released to atmosphere (0.1 and 0.33 kg t^{-1}, respectively). Acidification and freshwater ecotoxicity impacts are mainly a consequence of electricity and steam generation for the distillation train and absorption heat demands, respectively. These effects derive from emissions of NO_X and SO_2, as well as aluminized and chlorinated compound losses to water streams. Regarding the fossil sources depletion category, electricity and steam needs in the distillation unit are responsible for most of it. Remarkably, 3246 kg of natural gas is consumed per ton of maleic anhydride.

Regarding the production of maleic anhydride from furfural through partial oxidation in aqueous phase, the dehydration of maleic acid to MAN and the use of hydrogen peroxide (H_2O_2) as oxidant are the two main contributors to most of the impact categories (Figure 4B). Values listed in Table 5 evidence the larger impact on climate change caused by the MAN(a) process as compared to that achieved with the gas phase process, with a global warming potential (GWP) of almost 11 kg CO_2-equiv. kg^{-1} MAN, which is ≈10 kg more of CO_2-equiv. per kg of

Table 5. Total impacts of the gas phase and aqueous phase maleic anhydride production process from furfural, considering a gate-to-gate scope.

Environmental category	Unit	MAN(g)	MAN(a)
Acidification	Mole of H+ equiv.	0.13	7.26
Climate change	kg CO_2 equiv.	630.96	10994.56
Ecotoxicity, freshwater	CTUe	117.9	118883.5
Human toxicity, cancer	CTUh	3.16E−04	2.68E−06
Human toxicity, non-cancer	—	4.07E−05	2.19E−04
Land use	Pt	47.37	8714.64
Resource use, fossils	MJ	3003.64	197582.62
Water use	m^3 world equiv.	8.01	1364.73

maleic anhydride produced. Here again, fossil carbon is responsible for >99% of the climate change effects, and the greatest contributors are H_2O_2 use and the heat requirements for dehydration, with 4 and 6.23 t of CO_2 t^{-1} MAN emitted, respectively. Regarding the rest of the categories, despite the use of a large flow of process water that has a remarkable impact itself (1282.54 m^3 world-equiv., 94% of WU category), the major environmental drawback for this process arises from the dehydration of the reaction products stream. Removing large volumes of water (≈30 t t^{-1} MAN, Table S8, Supporting Information) implies a great energy cost, as evidenced in Figure 4B. Heating requirements imply a characterized impact of 110.6 GJ t^{-1} only in the transformation of maleic acid to maleic anhydride. This also has consequences in other categories such as acidification (4.17 mol H^+ per t) or freshwater ecotoxicity (9.57 CTUe per t). On the other hand, the use of hydrogen peroxide has notable implications in acidification because of large NO_X emissions (3.01 kg t^{-1}), in human toxicity through mercury loss (1.25 g t^{-1}), and in fossil depletion due to large consumption of natural gas, hard coal, and uranium (Supporting Information), all these features caused during the synthesis of H_2O_2.

Regarding the results listed in Table 5, the gas phase route seems more viable from an environmental perspective. All the studied indicators presented a lower value for this production alternative, with the only exception of the toxicity effects previously discussed. Thus, impact reduction seems to be easier in the gas phase MAN production process, as the main issue, the gas emissions in the absorption column, is isolated and these could be, at least, partially alleviated with an ad hoc treatment unit.

Aiming to integrate LCA and ExA conclusions within the same system boundaries, **Table 6** summarizes the results obtained for both processes regarding GWP, FD, and exergetic efficiency (ε_k). These indicators are selected to provide comparable data with the exergy analyses. From these results, the existence of a direct correlation between environmental impacts on climate change and fossil depletion is evident, with the energy requirements rather than with exergetic efficiency. Considering as examples the distillation unit in the purification stage of the gas phase process (T-101) and the heat exchanger E-102, the first unit shows a thermal efficiency of >99%, whereas heater E-102 has an efficiency below 70%. Unconcernedly, GWP and FD results are 645.5 and 689 times higher for the distillation unit, which is in line with the higher energy requirements of the column (7542.8 MJ t^{-1} for T-101, as compared to 38.2 MJ t^{-1} for E-102). Similarly, the reaction step is not very efficient from the exergy perspective (61.3% for MAN(g) and 14.5% for MAN(a)) but given its exothermic nature, no impacts on climate change or fossil depletion can be associated with it, since these do not consume fuels or any other energy source.

3.2.2. Cradle-to-Gate Boundaries

In this section, the system boundaries for the MAN production processes are expanded to explore the contribution of raw materials and furfural production to environmental impacts. For this purpose, furfural impact share is included within the analysis in a first term. Afterward, and due to its relevance, the main hotspots of furfural production are described. It must be noted that furfural quality requirements differ for MAN(g) and MAN(a) processes. In the case of the aqueous phase route, furfural can be used directly to produce maleic anhydride without the need for purification by the double azeotropic distillation (Section 2.3.3). Thus, impacts arising from this part of the process are avoided for the MAN(a) technology.

Figure 5 show the impacts of maleic anhydride production from furfural, both for MAN(g) and MAN(a) processes, respectively. The impacts introduced by the use of furfural as starting material in the overall processes are striking, particularly in the gas phase. In MAN(g) process, except for human toxicity category, which is still nearly exclusively caused by the furan emissions produced during the absorption phase, the rest of the categories are caused in a major proportion (>93%) by the impacts ascribed to furfural production. The importance of the contribution to the overall environmental impact of MAN

Table 6. Impacts on Climate Change and Fossil Depletion environmental categories comparison with thermal efficiency of unit operations within MAN(g) and MAN (a) process.

Unit	Category 1	Magnitude	Category 2	Magnitude	ε_k [%]
Gas phase process (MAN(g))					
E-100	Climate change (Kg CO_2-equiv.)	7.63	Fossil depletion [MJ]	121.14	75.8
E-101		2.18		34.65	97.4
E-102		0.93		14.9	68.6
T-100		484.28		504.79	99.9
T-101		601.6		10197.34	99.9
Aqueous phase process (MAN(a))					
E-200	Climate change (Kg CO_2-equiv.)	46.49	Fossil depletion [MJ]	787.26	23.4
E-201	–	18.41	–	311.77	61.2
T-200	–	6580.62	–	112666.15	51.0
T-201	–	42.33	–	716.92	30.1
T-202	–	4.71	–	79.76	12.0
T-203	–	41.92	–	709.79	53.4

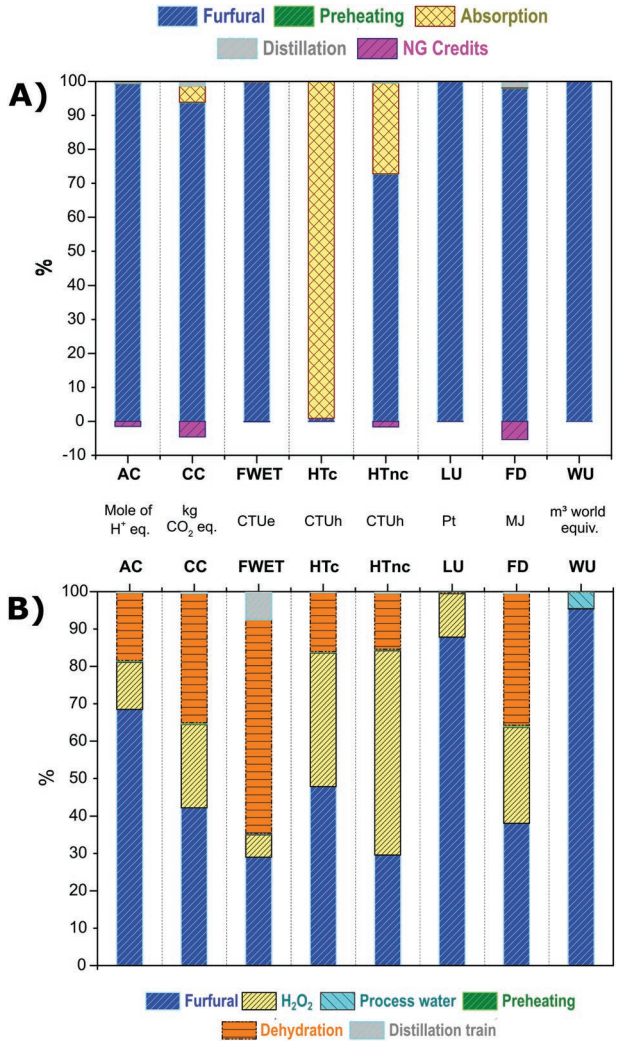

Figure 5. Relative contribution of A) gas and B) aqueous phase maleic anhydride production process from furfural to the analyzed impact categories, considering a cradle-to-gate scope. Negative values correspond to MP-Steam credits.

production through furfural oxidation can be easily assessed in the fossil depletion category. Thus, when furfural is kept out of the scope of the LCA study, credits from MP-Steam production imply an impact reduction up to 72% for the fossil depletion category. Including furfural manufacture reduces the avoided energy (MJ) to 5% of the overall process, due to the highly energy demanding furfural production processes. Similarly, acidification and global warming reduction are constrained from 69% to 1.5% (H^+ moles) and from 42% to 6% (Kg of CO_2-equiv.), respectively, when including furfural production within the LCA system boundaries.

In the case of the MAN(a) process, environmental impacts are far more distributed between furfural production and the maleic anhydride manufacture process. Nevertheless, furfural relative contribution still exceeds 50% of the total in 10 out of 16 indicators, including acidification and water use (Supporting Information). This is in accordance with the results observed in the previous section (Section 3.2.1.) as the burdens associated with the H_2O_2 use and the heat duties in the aqueous process make this route more unfavorable from an environmental perspective. The impact introduced by steam generation for stripping and heating purposes within furfural and maleic anhydride production has a similar effect on climate change and fossil depletion categories for both processes. However, the dehydration step within MAN(a) is still responsible for almost 59% of the freshwater eutrophication, and oxygen peroxide produces 57% of human non-cancer effects.

To avoid redundancies, given that results of the maleic anhydride manufacture have already been discussed, separate furfural data are disclosed to gain a deeper insight into its contribution to the overall MAN production process. Consequently, **Figure 6** shows the disaggregated results of the furfural production process, from farming stage to its delivery as input at the maleic anhydride factory gate. Two sub-processes are highlighted, namely maize production (i.e., corn cobs) and steam generation for process heating requirements. Besides, allocation plays a major role, as shipping furfural from China (the major producer of furfural worldwide) to its use in Europe also implies a significant burden over several categories, including acidification, freshwater ecotoxicity, and water use (Supporting Information).

Hereafter, the critical process aspects affecting the studied environmental categories are discussed in detail, aiming to understand its implications in maleic anhydride production. First, the acidification effects mainly arise from three sub-processes: cultivation, steam generation, and transportation. Cultivation impacts are related to emissions of ammonia (1.56 kg t^{-1}furfural) derived from the application of fertilizers. Nitrogen oxides (NO_X) and sulfur dioxide (SO_2) emissions during steam generation and transportation play an important role at this point because of the consumption of fuels in these subprocesses.

Impacts on climate change are, to a great extent (>80%), related to heat requirements, both for reaction and subsequent

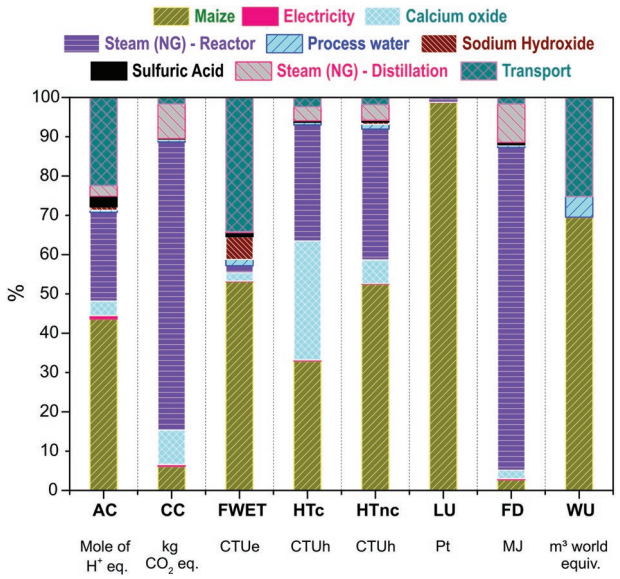

Figure 6. Relative contribution of the furfural production from corn cobs to the analyzed impact categories, considering a cradle-to-gate scope.

azeotropic distillation. In the Huaxia process (Section 2.3.3), biomass decomposition is produced by acid hydrolysis, in which pentoses (xylose and arabinose) evolving from the hydrolysis of the hemicellulosic fraction of biomass, undergo a dehydration pathway to furfural. Temperature conditions for the chemical transformations (≈155 °C) are provided by steam injection, which also serves for the separation of furfural from the reaction medium, first through a stripping step, and then in distillation towers to separate the azeotrope formed by water and furfural.[34] The high amount of steam required in the Huaxia process needs a huge consumption of fuel. If natural gas is used, this leads to the observed climate change effect (4644 kg CO_2-equiv. t^{-1} furfural). This negative effect can eventually be much worse considering other fuels, whose use is more widespread in PRC, where the furfural production plant would be allocated. In fact, biogenic carbon contribution is insignificant compared with the carbon originating from fossil sources. If mass allocation is not applied for the corn cob contribution, NO_X emitted during maize cultivation has a significant effect, as almost 40% of the impact category would be attributable to cultivation and harvesting of maize (Supporting Information).

Cultivation and harvesting of the maize also has a significant impact on the freshwater ecotoxicity. The main effects are related to the discharge of inorganics (chlorinated elements and ammonia), organics (chloroacetic acid and metolachlor), and metals (aluminum, copper, and nickel among others) to freshwater. In addition, wet deposition of emissions of these compounds presents a notable impact contribution. The large impact shown by transportation relates to the emission of 0.032 Kg of aluminum to freshwater per metric ton of furfural, which due to its importance on the USEtox model (characterization factor = 409000), leads to an impact factor of 13090.48 CTUe t^{-1} furfural.[42,43]

The human toxicity effects, both cancer and non-cancer related, are occasioned by maize cultivation, steam generation, and lime production for the neutralization of acid streams. Although their contribution is notable, regarding the absolute scores shown in Table S19, Supporting Information, no significant effects might be expected in comparison with the contribution of furan during MAN production in gas phase. Regarding the land use category, maize cultivation generates ≈99% of the impact. Arable and non-irrigated lands are especially affected.

3.2.3. Comparison Against Conventional Processes

Bearing in mind the previously described considerations and in order to explore the benefits of using a renewable feedstock, such as furfural, for MAN production, the gas and aqueous phase MAN production processes from furfural have been compared to current petrochemical technologies. The current production of maleic anhydride lies on two different technologies, based on the oxidation of two petrochemical feedstock: benzene or n-butane, with the second one being the most widespread.[44] Extensive information about both processes can be found elsewhere.[45,46] Putting the obtained results from the evaluation of the MAN(g) and MAN(a) cases in context is vital to ascertain the strengths of the technology and the improvements needed to tackle. In this sense, a comparison with benchmark pathways is established hereafter. **Table 7** compares the impact factor obtained for novel and conventional processes. Accounting for the sixteen environmental categories included in the EF 3.0, maleic anhydride produced from benzene yields the best results for 44% of the analyzed indicators, including acidification, human toxicity, and land use, although it yields significantly worse results in the categories of climate change and fossil consumption compared to the current leading process MAN(bt). Opposite to it, aqueous phase MAN production from furfural presents the worst results, yielding the highest impact in seven categories, with special clearance for climate change and fossil depletion effects. Gas-phase MAN production from furfural causes the lowest impact in three categories (e.g., freshwater ecotoxicity) and the highest in other three (e.g., human cancer effects). Slightly worse is the case of MAN production from butane, which originates the worst effects in six environmental categories (e.g., water use). On the other hand, supported by the large credits taken for the MP-steam production, this process shows the lowest fossil resources depletion effects.

Notwithstanding, in Section 3.2.2, the environmental burden allocation to the furfural production process was revealed as

Table 7. Impact scored by novel (MAN(g) and MAN(a)) and conventional (MAN(bn) and MAN(bt)) processes in the evaluated environmental categories using a cradle-to-gate scope.

	AC	CC	FWET	HTc	HTnc	LU	FD	WU
	Mole of H^+ equiv.	kg CO_2 equiv.	CTUe	CTUh	CTUh	Pt	MJ	m^3 world equiv.
Cradle-to-gate scope								
MAN(g)	18.77	10130.39	57576.85	3.18E–04	1.49E–04	74453.31	1.47E + 05	3.34E + 04
MAN(a)	21.25	17452.77	126660.52	4.32E–06	2.99E–04	73619.49	2.86E + 05	2.68E + 04
MAN(bn)	10.55	3702.73	3.77E + 05	1.18E–06	1.56E–05	1310.81	6.45E + 04	1.34E + 05
MAN(bt)	23.16	1050.74	5.15E + 05	1.39E–06	1.81E–05	1673.55	–1.39E + 03	2.38E + 05
Gate-to-gate scope								
MAN(g)	0.13	630.96	117.9	3.16E – 04	4.07E – 05	47.37	3003.64	8.01
MAN(a)	7.26	1.10E + 04	1.19E + 05	2.68E – 06	2.19E – 04	8714.64	197582.62	1364.73
MAN(bn)	1.86	1488.03	2.99E + 05	6.60E – 07	1.19E – 05	1300.07	–7169.13	1.29E + 05
MAN(bt)	3.56	979.74	5.14E + 05	1.06E – 06	1.74E – 05	1673.55	–1391.91	2.30E + 05

the major contributor to the impact generation in novel processes, especially in the MAN(g) scenario. Thus, the environmental results comparison of the maleic anhydride production processes are masked by the raw material results. In turn, if a gate-to-gate scope is considered (i.e., furfural, benzene, and n-butane are excluded from the analysis), the output data change radically. From this perspective, the best-case scenario indisputably corresponds to the gas phase process from furfural, which yields the best results in thirteen out of sixteen categories. MAN(a) on the other hand, although achieving a pronounced impact reduction, still leads to the worst effects in half of the evaluated indicators, including the five in Table 7. Nevertheless, the conventional technologies such as benzene or butane to MAN are already mature, and no significant optimization can be easily introduced, while the alternative processes evaluated within this study have ample room for improvement. In this sense, the impact reduction introduced by subtracting the furfural from the analysis is much higher compared to the effect of benzene and n-butane reduction. Thus, changes in furfural production could lead to an average impact decrease of up to 60% in the case of MAN(a) (Table S22, Supporting Information). On the other hand, downstream optimization in the conventional technologies could lead to a potential reduction of 43% of the impact in the case of the benzene process and 24% in the case of the butane process.

In conclusion, among conventional processes, the benzene pathway achieves better results in several LCA impact categories, although it is far from the n-butane pathway when referring to some critical aspects (i.e., climate change and fossil depletion effects), a fact also acknowledged by previous studies.[26] Regarding the alternative processes based on the oxidation of furfural, gas-phase production of MAN comprehensively over-performs the aqueous phase process in environmental terms. MAN(a) is still distant to yield competitive environmental results, and further changes need to be introduced relative to the oxidant agent and the dehydration energy requirements. Comparing the conventional MAN and MAN(g) alternatives, the petrochemical routes seem to imply slight benefits with regards to the novel process but this could be easily turned around if two conditions are met. First, the absorption effluent from MAN(g) containing furan should be treated to reduce toxicity effects. Second, the furfural production process needs to be optimized in terms of energy requirements and maize cultivation.

4. Conclusion

Exergoeconomic and environmental analyses have been applied to two maleic anhydride production processes using furfural as the raw material: one based on the use of air as oxidant and gas phase operating conditions, and another one using H_2O_2 as oxidant, liquid phase operating conditions, and water as the reaction medium. The results of both studies are unequivocal in pointing out the aqueous phase process as the least indicated to undertake the transformation from energy and environmental points of view. The highly inefficient use of energy, together with the use of the highly toxic H_2O_2 as oxidant, conduct to this poor evaluation. In contrast, the gas phase MAN production process from furfural, despite requiring the initial vaporization of the feedstock, does not show many weaknesses from an energy point of view, though there is some room for improvement from an environmental perspective, especially regarding gas emissions. Expanding the system boundaries to include the starting feedstock and furfural production within the analyses led to an interesting conclusion: the production of furfural accounts for the major contribution to the environmental impacts, regardless of the technology used for oxidation. This result arises from the highly environmentally inadequate technologies conventionally used to produce furfural (e.g., the Huaxia process). This fact makes the environmental footprint of MAN production processes, even if conducting in gas phase conditions and using air as oxidant, comparable to that provided by petrochemical technologies, such as those using benzene or butane as feedstock. Nevertheless, these latter options are well developed highly optimized production processes, whereas the biomass derived furfural-based MAN production processes still show a high potential for improvement. Making use of exergoeconomic and environmental analysis to point out the weaknesses for these processes is an excellent first step for their improvement.

Supporting Information

Supporting Information is available from the Wiley Online Library or from the author.

Acknowledgements

This research was funded by the Spanish Ministry of Science, Innovation and Universities (projects RTI2018-094918-B-C41, RTI2018-094918-B-C42, and RTI2018-094918-B-C43).

Conflict of Interest

The authors declare no conflict of interest.

Data Availability Statement

The data that support the findings of this study are available from the corresponding author upon reasonable request.

Keywords

environmental impacts, exergoeconomic analysis, furfural, life cycle analysis, maleic anhydride

Received: March 15, 2022
Revised: May 22, 2022
Published online: June 22, 2022

[1] IPCC, Assessment Report 6 Climate Change 2021: The Physical Science Basis **2021**.

[2] J. Popp, S. Kovács, J. Oláh, Z. Divéki, E. Balázs, *New Biotechnol.* **2021**, *60*, 76.
[3] A. Aguilar, T. Twardowski, R. Wohlgemuth, *Biotechnol. J.* **2019**, *14*, e1800638.
[4] IEA Bioenergy, The Availability of Biomass Resources for Energy: Summary and Conclusions from the IEA Bioenergy ExCo58 Workshop, IEA Bioenergy: ExCo2008:02 **2008**.
[5] B. Kamm, M. Kamm, P. R. Gruber, S. Kromus in *Biorefineries-Industrial Processes and Products: Status Quo and Future Directions* (Eds: B. Kamm, P. R. Gruber, M. Kamm), Vol. 1, Wiley-VCH, Weinheim, Germany **2006**, Ch. 1.
[6] J. C. Solarte-Toro, C. A. Cardona Alzate, *Bioresour. Technol.* **2021**, *340*, 125626.
[7] R. S. Barker (Scientific Design Co Inc), *US3867412*, **1975**.
[8] R. A. Mount, H. Raffelson (Huntsman Specialty Chemicals Corp, Bankers Trust Co), *US4111963*, **1978**.
[9] A. Chatzidimitriou, J. Q. Bond, *Green Chem.* **2015**, *17*, 4367.
[10] N. Alonso-Fagúndez, M. L. Granados, R. Mariscal, M. Ojeda, *ChemSusChem* **2012**, *5*, 1984.
[11] Y. Rodenas, R. Mariscal, J. L. G. Fierro, D. Martín Alonso, J. A. Dumesic, M. López Granados, *Green Chem.* **2018**, *20*, 2845.
[12] I. Agirre, I. Gandarias, M. L. Granados, P. L. Arias, *Biomass Convers. Biorefin.* **2020**, *10*, 1021.
[13] D. Fytili, A. Zabaniotou, *Curr. Opin. Green Sustainable Chem.* **2017**, *8*, 5.
[14] N. Escobar, N. Laibach, *Renewable Sustainable Energy Rev.* **2021**, *135*, 110213.
[15] J. Moreno, C. Pablos, J. Marugán, in *Quantitative Methods for Food Safety and Quality in the Vegetable Industry* (Eds: F. Perez-Rodríguez, P. Skandamis, V. Valdramidis), Springer International Publishing, Cham, Switzerland **2018**, Ch. 12.
[16] G. Tsatsaronis, F. Cziesla, in *Encyclopedia of Physical Science and Technology* (Ed: R. A. Meyers), Academic Press, **2003**, p. 659, https://doi.org/10.1016/B0-12-227410-5/00944-3.
[17] M. Aghbashlo, Z. Khounani, H. Hosseinzadeh-Bandbafha, V. K. Gupta, H. Amiri, S. S. Lam, T. Morosuk, M. Tabatabaei, *Renewable Sustainable Energy Rev.* **2021**, *149*, 111399.
[18] J. Wu, N. Wang, *J. Environ. Manage.* **2021**, *296*, 113151.
[19] T. A. Z. de Souza, D. H. D. Rocha, A. A. V. Julio, C. J. R. Coronado, J. L. Silveira, R. J. Silva, J. C. E. Palacio, *J. Cleaner Prod.* **2021**, *311*, 127577.
[20] M. Finkbeiner, A. Inaba, R. Tan, *Int. J. Life Cycle Assess.* **2006**, *11*, 80.
[21] European Commission, *Joint Research Centre, Institute for Environment and Sustainability, International Reference Life Cycle Data System (ILCD) Handbook – Reviewer qualification for Life Cycle Inventory data sets*, EUR 24379 EN, Luxembourg, Publications Office of the European Union, **2010**.
[22] S. Soltanian, M. Aghbashlo, S. Farzad, M. Tabatabaei, M. Mandegari, J. F. Görgens, *Renewable Energy* **2019**, *143*, 872.
[23] K. Wiranarongkorn, K. Im-orb, J. Panpranot, F. Maréchal, A. Arpornwichanop, *Energy* **2021**, *226*, 120339.
[24] C. Lythcke-Jørgensen, F. Haglind, L. R. Clausen, *Energy Convers. Manage.* **2014**, *85*, 817.
[25] J. Q. Albarelli, S. Onorati, P. Caliandro, E. Peduzzi, M. A. A. Meireles, F. Marechal, A. V. Ensinas, *Energy* **2107**, *138*, 1281.
[26] P. V. Mangili, D. M. Prata, *Chem. Eng. Sci.* **2020**, *212*, 115313.
[27] J. Szargut, *Exergy Method: Technical and Ecological Applications*, WIT Press, Southampton, UK **2005**.
[28] R. Rivero, M. Garfias, *Energy* **2006**, *31*, 3310.
[29] A. Lazzaretto, G. Tsatsaronis, *Energy* **2006**, *31*, 1257.
[30] H. Schöppe, P. Kleine-Möllhoff, R. Epple, *Processes* **2020**, *8*, 119.
[31] Wondu Business and Technology Services. *Furfural chemicals and biofuels from agriculture*. Rural Industries Research and Development Corporation, **2006**.
[32] M. Dashtban, A. Gilbert, P. Fatehi, *J. Sci. Technol. For. Prod. Processes* **2012**, *2*, 44.
[33] D. T. Win, *AU. J. Technol.* **2005**, *8*, 185.
[34] K. J. Zeitsch, *The Chemistry and Technology of Furfural and Its Many By-Products*, 1st ed., Sugar Series, Vol. *13*, Elsevier, Amsterdam, the Netherlands **2000**, Ch. 11.
[35] European Commission, *European Comission, Directorate General for Internal Market, Industry, Entrepreneurship and SMEs. Taking bi-based from promise to market. Measures to promote the market introduction of innovative bio-based products*, **2010**.
[36] K. H. Kromer, M. Martinov, *Landtechnik* **1981**, *36*, 412.
[37] S. Soltanian, M. Aghbashlo, F. Almasi, H. Hosseinzadeh-Bandbafha, A.-S. Nizami, Y. S. Ok, S. S. Lam, M. Tabatabaei, *Energy Convers. Manage.* **2020**, *212*, 112792.
[38] A. A. Vitoriano Julio, E. A. Ocampo Batlle, C. J. Coronado Rodriguez, J. C. Escobar Palacio, *Waste Biomass Valorization* **2021**, *12*, 5611.
[39] Y. Casas Ledón, P. González, S. Concha, C. A. Zaror, L. E. Arteaga-Pérez, *Energy* **2016**, *114*, 239.
[40] X. Jian, J. Li, Q. Ye, L. Yan, X. Li, L. Xie, J. Zhang, *Sep. Purif. Technol.* **2022**, *287*, 120499.
[41] A. Crivellari, V. Cozzani, I. Dincer, *Energy* **2019**, *187*, 115947.
[42] M. Z. Hauschild, R. K. Rosenbaum, S. I. Olsen, *Life Cycle Assessment: Theory and Practice*, Springer, Berlin **2017**.
[43] M. Z. Hauschild, M. Huijbregts, O. Jolliet, M. Macleod, M. Margni, D. Van De Meent, R. K. Rosenbaum, T. E. McKone, *Environ. Sci. Technol.* **2008**, *42*, 7032.
[44] B. C. Trivedi, B. M. Culbertson, *J. Polym. Sci.* **1983**, *21*, 958.
[45] D. Lesser, G. Mestl, T. Turek, *Chem. Eng. Sci.* **2017**, *172*, 559.
[46] J. Maußner, H. Freund, *Chem. Eng. Sci.* **2018**, *192*, 306.